Science of Sintering, **54** (2022) 495-506

https://doi.org/10.2298/SOS2204495R

UDK: 553.611; 622.785; 553.08

Fabrication of Ceramic Monoliths from Diatomaceous Earth: Effects of Calcination Temperature on Silica Phase Transformation

Arianit A. Reka[1,2,3*)], Darko Kosanović[2,4], Egzon Ademi[1], Patrick Aggrey[5], Avni Berisha[3], Blagoj Pavlovski[6], Gligor Jovanovski[7], Besnik Rexhepi[1], Ahmed Jashari[1], Petre Makreski[8]

[1]Faculty of Natural Sciences and Mathematics, University of Tetovo, Ilinden str. n.n., 1200 Tetovo, North Macedonia,
[2]Department of Materials Science and Engineering, Missouri University of Science and Technology, Rolla, MO 65409, USA
[3]NanoAlb-Unit of Albanian Nanoscience and Nanotechnology, Albanian Academy of Sciences, Tirana, Albania
[4]Institute of Technical Sciences of the Serbian Academy of Sciences and Arts, Knez Mihailova 35/IV, 11000 Belgrade, Serbia
[5]Hierarchically Structured Materials, Center for Energy Science and Technology, Skolkovo Institute of Science and Technology, Nobel Street 3, 121205, Moscow, Russia
[6]Faculty of Technology and Metallurgy, Ss. Cyril and Methodius University in Skopje, Ruger Boskovic bb, 1000 Skopje, North Macedonia
[7]Macedonian Academy of Sciences and Arts, Research Center for Environment and Materials, Bul. Krste Misirkov 2, 1000, Skopje, North Macedonia
[8]Institute of Chemistry, Faculty of Natural Sciences and Mathematics, Ss. Cyril and Methodius University in Skopje, Arhimedova 5, 1000 Skopje, North Macedonia

Abstract:

The raw diatomaceous earth from the vicinity of Bitola (North Macedonia) showed low bulk density (0.61–0.69 g/cm^3), high-water absorption (75–81%) and porosity (66–72%). The chemical composition was determined with ICP-MS, revealing the following results for the diatomaceous earth: SiO_2 (63.69 wt%), Al_2O_3 (11.79 wt%), Fe_2O_3 (5.95 wt%), MnO (0.15 wt%), TiO_2 (0.65 wt%), CaO (1.51 wt%), MgO (2.24 wt%), P_2O_5 (0.13 wt%), K_2O (1.64 wt%), Na_2O (0.93 wt%), LOI (11.21 wt%). XRPD data of the examined sample of clayey diatomite mainly depicted crystalline behavior with a small presence of amorphous phase. The crystalline mineral phases mainly comprise: silica (quartz), feldspars (plagioclase), mica (muscovite), chlorites and dolomite. SEM and TEM results show cased presence of micro- and nanostructures with pores ranging from 250 to 600 nm. The clayey diatomite was sintered at three temperatures (900, 1000 and 1100ºC) for a period of 1 h. XRPD of the sintered samples at 1100ºC showed certain thermal stability and formation of new phases (mullite and tridymite) that makes the analyzed diatomaceous earth suitable for production of various types of ceramic, construction and thermal insulating materials.

Keywords: *Diatomaceous earth; Clay minerals; Characterization; Sintering.*

*) **Corresponding author:** arianit.reka@unite.edu.mk

1. Introduction

North Macedonia is abundant in natural inorganic non-metallic materials with a wide spectrum of potential use and application, such as diatomaceous earth (DE), perlites, bentonites, pumice, dolomite, granite, quartzite, etc. [1-10]. The clayey DE found in the proximity of the Bitola power plant, takes a special place amongst non-metallic raw materials. It represents a mixture of diatomite and clay minerals. It constitutes a biogenetic rock; grayish, soft, very light, weakly cemented, finely opal sedimentary rock [11-19].

Diatomaceous earths are composed mainly of accumulated remains of skeletons [20] and are considered to be a natural nano materials [21], with various uses and applications such as: filtration material, purification of industrial waters and absorption material in an industrial scale [22-24], used as catalyst support [25], glass industry [26], production of porous ceramics [27-34], as pozzolanic material in the cement industry, pesticide holder, for improving the physical and chemical characteristics of certain soils [35-41], for production of humidity control materials [42], initial material for production of prolonged-release drug carriers [43], as a filler in plastics and paints [44], and many other uses.

Taking in consideration that the DE is mined from geological deposits, it may contain certain impurities such as metal oxides and organic matter. The chemical composition of diatomaceous earth is predominantly silica (SiO_2) while the impurities are Al_2O_3, Fe_2O_3, CaO, MgO, K_2O, Na_2O, P_2O_5 and so on, which may have particular effects towards its application properties. One way to improve the properties of DE is through the sintering process. During the sintering process, the impurities are removed followed by mineralogical changes that results in the enhancement on the characteristics of diatomite [45-53].

In this study the impact of the sintering process on the silica phase transition in DE was analyzed. It was investigated how the DE and the clay minerals behave during sintering. The raw material is sintered at three temperatures 900, 1000 and 1100^{o}C for a period of one hour. The transition mechanisms of the occurring changes are discussed by means of XRPD.

2. Matherials and Methods

The clayey diatomite was collected from Bitola region, Republic of North Macedonia. The used material is considered a waste in North Macedonia and it is of utmost importance and significance to be valorized.

For the purpose of sintering, the DE was first crushed and ball-milled for a period of 2.5 h. After the pulverization of the material, the samples were sintered at three temperatures: 900, 1000 and 1100°C. The temperature was hold for 60 min at each temperature interval. The mineralogical composition was further subsequently analyzed by XRPD.

The determination of the chemical composition and the trace elements was performed with Inductively Coupled Plasma Mass Spectrometry (ICP-MS, Agilent 7500cx).

The mineralogical characterization of the DE was carried out by an X-ray powder diffraction (XRPD), thermal analysis (TGA/DTA), scanning electron microscopy (SEM-EDS), transmission electron microscopy (TEM) and infrared spectroscopy (IR).

XRPD analysis was performed on Rigaku Ultima IV X-ray diffractometer equipped with D/teXhigh-speed 1-dimenzional detector using Cu$K\alpha$ radiation (λ = 1.54178 Å) in 2θ range from 5 to 60°. The accelerating voltage and the current power were set to 40 kV and 40 mA, respectively.

DTA/TGA analyses of the clayey diatomite were performed in an air environment with Stanton Redcroft apparatus, under the following experimental conditions: temperature range from 20–1200°C; speed of heating set to 10°C/min; sample mass of 13.577 mg. The ceramic pot was used as a material carrier.

Scanning electron microscopy VEGA3 LMU coupled with energy dispersive X-ray spectroscopy (INCA Energy 250 Microanalysis System) was used to quantitative analyze the material. The accelerating voltage of the SE detector was set to 20 kV.

The Perkin-Elmer FTIR system 2000 interferometer was engaged to record the IR spectra in 4000–500 cm^{-1} range using the KBr pellet method. The pellets were prepared by a mixture of the sample (1 mg) with dried KBr (200 mg) pressed at 10 tcm^{-2}.

3. Results and Discussion

3.1. Physical-mechanical properties of diatomaceous earth

From the physical-mechanical perspective, the examined DE subject of this study represents a sedimentary rock (of biogenetic genesis) with grayish color, soft, loose and light material, with fine to superfine grained structure, porous, shell-like etc. The tested sample is easily disintegrated by applying pressure to it, while the fine particles give you the feeling of scratch. The characterization of the physical-mechanical properties of the raw material is performed by analyzing the compressive strength in dry state. The bulk density is determined in dry state as well. The bulk density is 0.61–0.69 g/cm^3, the density is 2.39 g/cm^3, while the compressive strength in natural state (raw) is 3.44 MPa. The physical-mechanical properties of DE are shown in Table I.

Tab. I Physical mechanical properties of the used diatomaceous earth.

Bulk density (g/cm^3)	Water absorption (%)	Density (g/cm^3)	Compressive strength (MPa)
0.61–0.69	75–81	2.39	3.44

3.2. Chemical analysis of diatomaceous earth

The chemical composition of the DE was analyzed by ICP-MS. The loss of ignition (LOI) was 11.29 %, obtained at 1000°C. The results from the chemical composition of DE indicate that the analyzed material is an acidic rock with presence of SiO_2 at 63.69 % and considerable content of Al_2O_3 (11.79 %) and Fe_2O_3 (5.95 %). Tabs II and III present the chemical composition of the major oxides and the trace elements, respectively.

Tab. II Chemical composition of diatomaceous earth.

Oxides	SiO_2	Al_2O_3	Fe_2O_3	MnO	TiO_2	CaO	MgO	P_2O_5	K_2O	Na_2O	LOI	**Total**
Mass (wt.%)	63.69	11.79	5.95	0.15	0.65	1.51	2.24	0.13	1.64	0.93	11.29	99.99

Tab. III Trace elements determined in the diatomaceous earth.

Trace element	Cu	Cr	Ni	Co	Zn	V	Pb	Cd	As	Se	Tl	Bi	Ba	Rb
Content (ppm)	112	109.5	41.1	22.5	3.61	113.1	10.28	0.59	5.89	3.19	0.89	0.56	459.4	114.5
Trace element	Sr	Cs	Th	U	Mo	Sn	Sb	Pd	Ag	Ga	Ge	Li	Be	B
Content (ppm)	166.2	4.19	9.58	7.67	1.59	2.77	0.19	0.59	2.49	16.58	1.01	32.69	2.59	<10

3.3. X-ray powder diffraction analysis of diatomaceous earth

As shown in Fig. 1 the XRPD pattern of the examined sample of natural DE mainly depicts crystalline behavior with a small presence of amorphous phase. The crystalline phases are mainly represented by silica (quartz), feldspars, mica (muscovite), chlorites and dolomite.

Tab. IV XRPD data of the raw diatomaceous earth.

Silica	**d(Å)**	4.25	3.34	2.45	2.28	1.81	1.54						
	(°)	20.88	26.65	36.57	39.51	50.16	59.79						
Feldspars	**d(Å)**	6.36	4.02	3.77	3.66	3.61	3.23	3.20	3.19	2.95	2.92		
(plagioclase)	**(°)**	13.90	22.05	23.55	24.30	24.65	27.51	27.83	27.96	30.25	30.50		
Mica	**d(Å)**	9.91	4.96	4.47	3.86	3.49	3.31	2.99	2.85	2.80	2.56	2.35	2.23
								2.12	1.98	1.97	1.73	1.67	1.65
(muscovite)	**(°)**	8.92	17.85	19.84	23.01	25.54	26.91	29.88	31.28	31.85	34.96	38.22	40.32
								42.49	45.56	45.96	52.92	54.93	55.35
Chlorites	**d(Å)**	14.10	7.05	4.70	3.53	2.59	2.49	2.38	2.31				
(clinochlore)	**(°)**	6.26	12.53	18.84	25.54	34.50	36.08	36.75	38.86				
Dolomite	**d(Å)**	2.89	2.67	2.19	1.80	1.78							
	(°)	30.85	33.48	41.14	50.61	51.17							

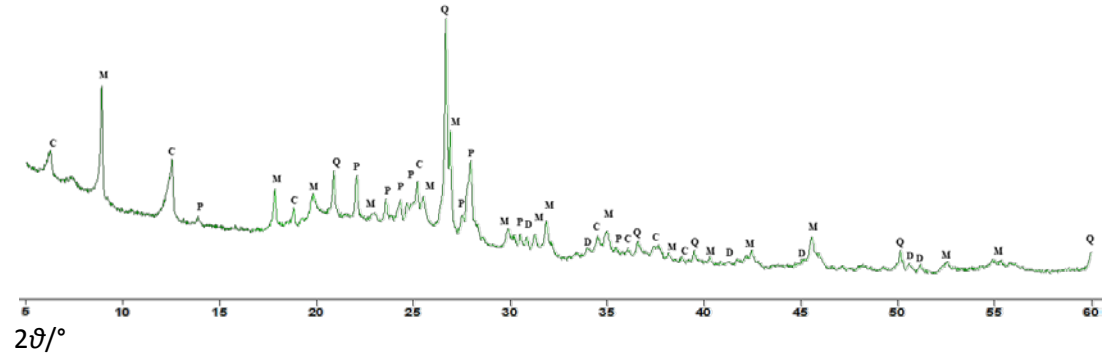

Fig. 1. XRPD diagram ofthe raw diatomaceous earth. The peak associated by each crystalline phase is marked (Q: quartz, M: muscovite, C: clinochlore, P: plagioclase, D: dolomite).

3.4. Infrared spectrum interpretation of the diatomaceous earth

The infrared bands of the raw DE exhibits the bands at 3697cm^{-1}, 3620 cm^{-1} and 760 cm^{-1} due to the presence of muscovite phase [54]. The evident broad band around 3429 cm^{-1} is attributed to the H–O–H stretching vibrations of absorbed water. The band at 1637 cm^{-1} occurs from the H–O–H bending vibrations of adsorbed water in the phyllosilicate (sheet silicate) minerals as well as from the H_2O present in opal-A. The band at 1039 cm^{-1} associated by the shoulder at 1100 cm^{-1} is attributed to the Si–O–Si stretching vibration [52]. The band at 796 cm^{-1} band is related to the OH translational vibration and Si–O–Si bending vibrations within the framework [52-53]. The dolomite presence in the DE is mapped by the band at 722 cm^{-1} from the $\nu_4(CO_3^{2-})$ vibration [54], whereas the bands at 694 and 745 cm^{-1} are due to the clay minerals in the sample [55]. The absorption bands around 648 cm^{-1} and 529 cm^{-1} originate from Si–O–Al vibrations (Al in octahedral coordination), while the band around 468 cm^{-1} is attributed to the Si-O-Si bending vibrations [23,41,51]. The bands centered at 424 cm^{-1} and 468 cm^{-1} appear from the presence of the feldspars in the sample [54].

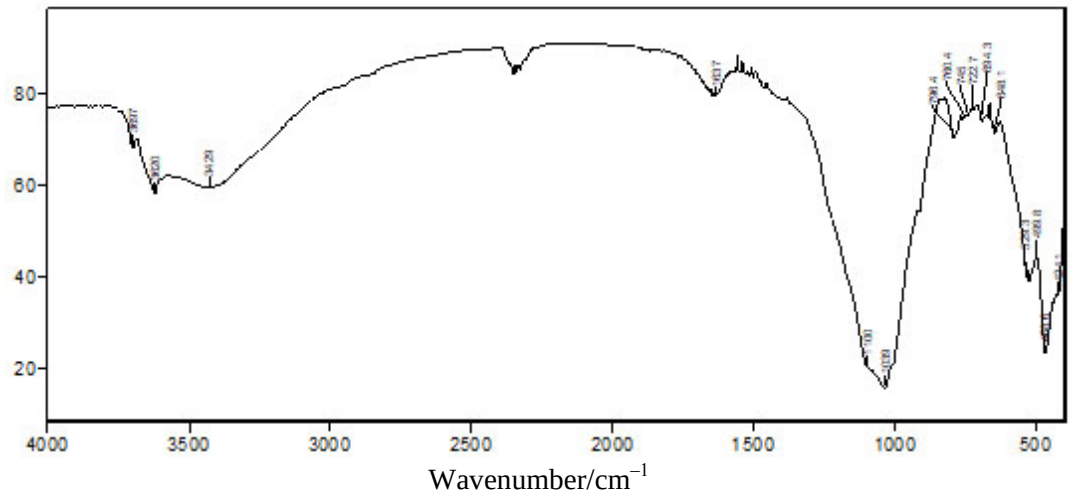

Fig. 2. IR spectrum of the raw diatomaceous earth.

3.5. Scanning electron microscopy (SEM) of diatomaceous earth

The scanning electron microscopy images of the DE provide (Fig. 3) illustrated the biogenic origin of the sample because of the presence of various skeletal forms. These skeletons are remains of diatom algae and exhibit morphology depicting clearly visible nanometric pores (300–650 nm). Despite their pronounced variation in size, volume and shape, they do not contain impurities and majority of them are open. The observed features give credit for this material to be suitable for use in various fields of the chemical industry (filter, absorbent, clarifier etc.).

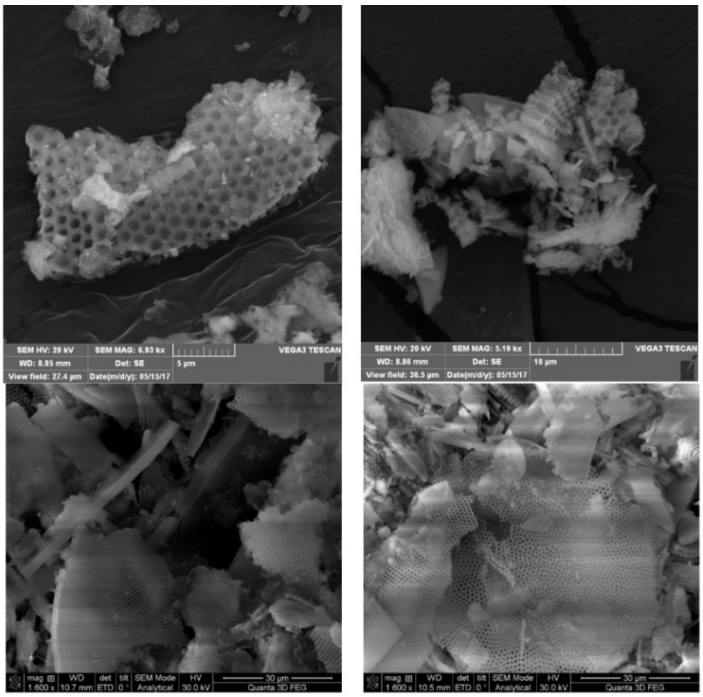

Fig. 3. SEM of DE composed of various micro-relics-skeletons of biogenic origin with various forms, with pores ranging from 300–650 nm. The well-preserved frustules with fine details indicating that the diagenetic alternations were not significant.

The employment of the SEM-EDX enabled to quantitatively determine the chemical composition of the DE. The element weight percentage (Fig. 4, O: 59.23%, Al: 2.52%, Si: 35.15%, K: 0.86%, Ca: 0.72%, Fe: 1.51%) confirms the presence of clay minerals in the sample.

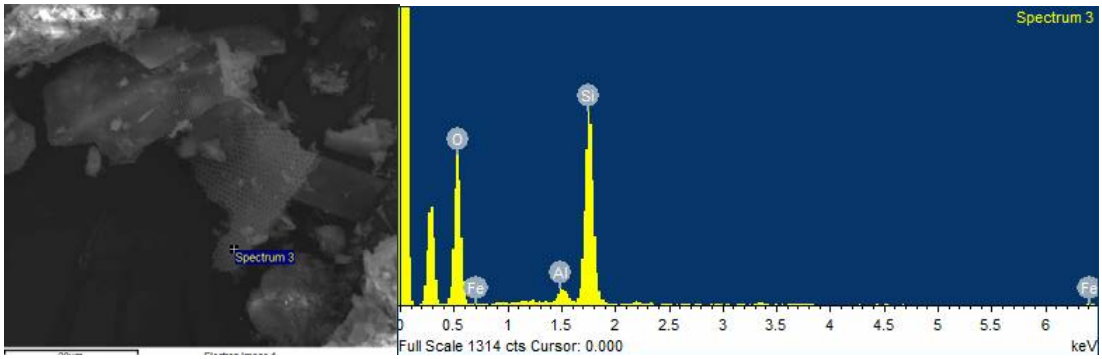

Fig. 4. SEM of DE (left) and the element content as determined by EDS (right).

3.6. Transmission electron microscopy (TEM) of the diatomaceous earth

The TEM results of the DE inferred that the analyzed sample confirms the results of the SEM analysis in regards to the texture and the morphology and especially the pore sizes found in the raw material (Fig. 5). The pore size ranges between 250–650 nm, but dominantly span within the 250–350 nm range. The diatom shells in DE show porous structure and somewhat clean surface, while pores are filled by impurities due to the clay minerals found in the sample.

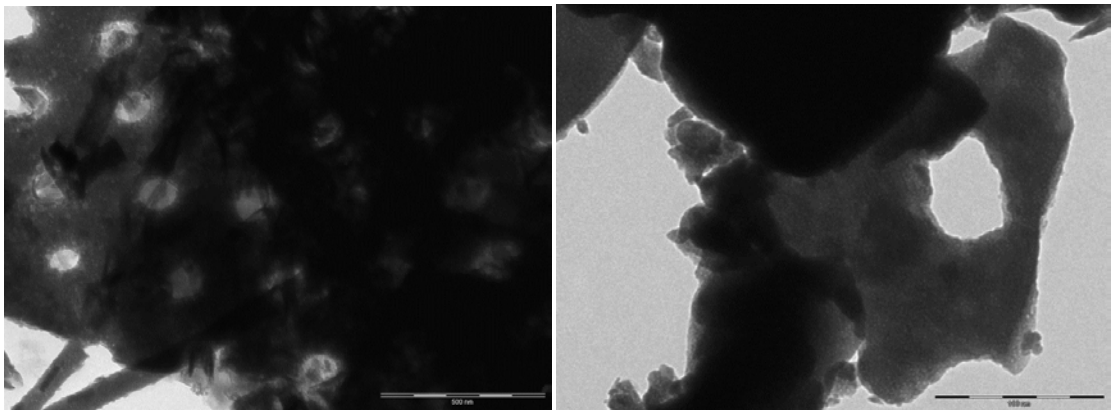

Fig. 5. TEM photomicrographs of the DE with visible pores ranging from 250 nm to 350 nm.

3.7. Compressive strength of sintered monoliths

The samples were prepared in semi-dry condition, using sufficient moisture in order to obtain cylindric monoliths. The samples were sintered at three temperature intervals: 900, 1000 and 1100°C. Based on the results (Table V), it is evident that the compressive strength of DE monoliths (Fig. 7) increases with the increase of the sintering temperature. Subsequently, the monoliths sintered at 900°C show compressive strength of 10.37 MPa, while the sintered at 1000 and 1100°C showed increased compressive strength of 14.56 MPa

and 22.78 MPa, respectively. These observed values of are comparable to other porous ceramics fabricated from comparatively more expensive starting materials.

Tab. V Physical-mechanical properties of cylinders of diatomaceous earth sintered at 900, 1000 and 1100°C for a period of 60 min.

Temperature (°C)	Bulk density (g/cm^3)	Compressive strength (MPa)	Mass (g)	Diameter (mm)	Shrinkage (%)
20	-	-	-	20.00	-
900	0.87	10.37	2.14	19.65	1.75
1000	0.95	14.56	2.16	19.26	3.70
1100	1.16	22.78	2.12	18.77	6.15

3.7. X-ray powder diffraction analysis of sintered diatomaceous earth

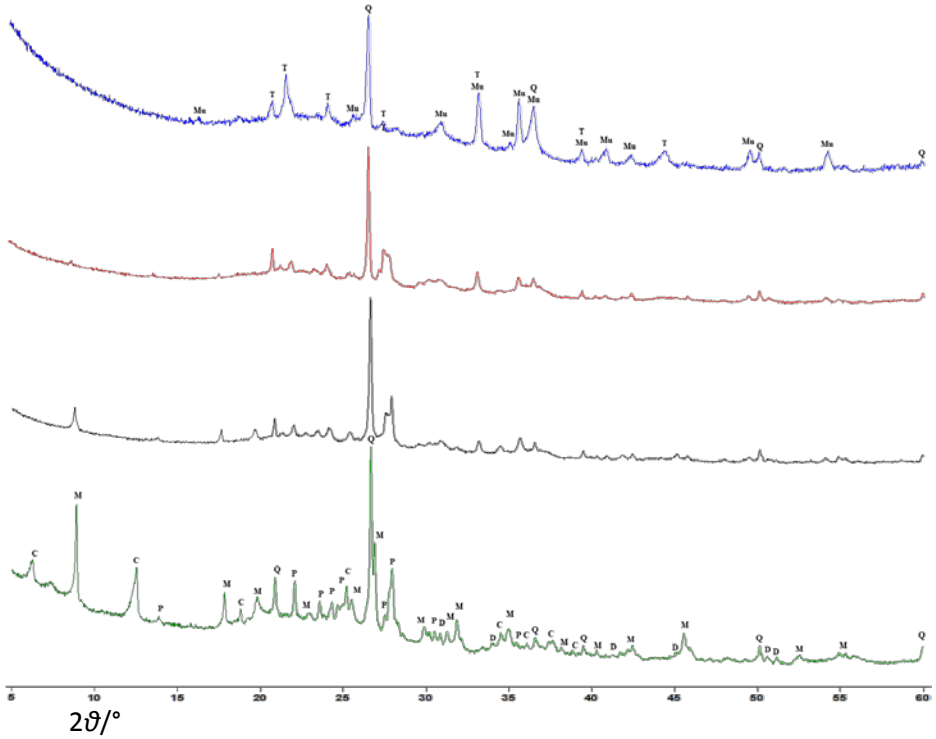

Fig. 6. XRPD analysis of raw DE (a), thermally treated sample for a period of 1 hr at 900°C (b), at 1000°C (c), at 1100°C (d).

As reported previously, the XRPD pattern of the examined sample of DE mainly depicted crystalline behavior with a small presence of amorphous phase (Fig. 6). The crystalline phases are mainly represented by silica (quartz), feldspars (plagioclase), mica (muscovite), chlorites and dolomite. The results of the XRPD analysis of the sintered DE at 900, 1000 and 1100°C showed that the amount of the amorphous phase was expanded as the temperature was increased. In the XRPD pattern of the sample sintered at 1100°C, the complex “bump” positioned between 17 and 20° (2θ) emerged. This “bump” is attributed to the transformation of the crystalline phase into aluminosilicate amorphous glass. During the sintering of the DE, a slight decrease of the quartz phase was observed (at 1100°C), and the formation of two new phases (mullite and tridymite) is apparent (see Table VI).

Tab. VI The peaks evolving in the XRPD pattern of diatomaceous earth sintered at 1100°C.

Mullite	*d*(Å)	5.40	3.44	3.39	2.88	2.69	2.55	2.51	2.28	2.20	2.13	2.04	1.83	1.69
	(°)	16.40	25.85	26.14	30.94	33.20	35.05	35.52	39.42	40.86	42.37	44.34	49.54	54.21
Tridymite	*d*(Å)	4.31	4.10	3.68	2.51	2.28	2.04							
	(°)	20.60	21.62	24.23	32.52	39.42	44.34							

4. Conclusions

The DE was found to represent a weakly bound, very soft loose rock with a greyish white color, with a low bulk density (0.61–0.69 g/cm^3), and high-water absorption (75-81%) and porosity (66-72%).

The microscopic analysis of the DE defines the biogenic origin of the material. Additionally, SEM and TEM results reveal presence of micro- and nanostructures with pores ranging from 250-600 nm.

From chemical as well as mineralogical point of view, either as raw or sintered, the DE represents a raw material with high potential use as adsorbent, production of filter media and catalyst. Compared to other naturally occurring nanocarriers, the nanometric size pores and morphology of these nanostructures found in the DE strengthen its potential for its use in drug delivery applications and/or for production of various composite materials.

The overall pool the presented results provide valuable information regarding the nature of raw DE its sintering behavior in the interval 900–1100°C. The thermal stability, and particularly the phase transformations during the sintering, is of significant importance for its use and application. The formation of mullite and tridymite at 1100°C classified the material as suitable for production of various types of ceramic materials (different construction materials and thermal insulating materials).

Acknowledgments

Authors thank the Ministry of Education and Science of North Macedonia for the financial support. Funds for the realization of this work are provided by the Ministry of Education, Science and Technological Development of the Republic of Serbia, Agreement on realization and financing of scientific research work of the: Institute of Technical Sciences of SASA in 2022 (Record number: 451-03-68/2022-14/200175).

5. References

1. Spasovski O., Spasovski D., The potential of the nonmetallic mineral resources in the Republic of Macedonia, Geologica Macedonica, 26 (2012) 91-94.
2. Makreski P., Jovanovski G., Kaitner B., Minerals from Macedonia. XXIV. Spectra-structure characterization of tectosilicates, Journal of Molecular Structture, 924-926 (2009) 413-419.
3. Jovanovski G., Boev B., Makreski P., Minerals from the Republic of Macedonia with an Introduction to Mineralogy, Macedonian Academy of Sciences and Arts, Skopje, (2012) 1–652.
4. Reka A.A., Pavlovski B., Lisichkov K., Jashari A., Boev B., Boev I., Lazarova M., Eskizeybek V., Oral A., Jovanovski G., Makreski P., Chemical, mineralogical and structural features of native and expanded perlite from Macedonia, Geologia Croatica, 72 (2019) 215-221.

5. Memedi H., Atkovska K., Lisichkov K., Marinkovski M., Kuvendziev S., Bozinovski Z., Reka A.A., Removal of Cr(VI) from water resources by using different raw inorganic sorbents, Quality of life, 7 (2016) 77-85.
6. Memedi H., Atkovska K., Lisichkov K., Marinkovski M., Kuvendziev S., Bozinovski Z., Reka A.A., Separation of Cr(VI) From Aqueous Solutions by Natural Bentonite: Equilibrium Study, Quality of Life, 8 (2017) 41-47.
7. Memedi H., Atkovska K., Lisichkov K., Marinkovski M., Bozinovski Z., Kuvendziev S., Reka A.A., Jakupi S., Application of natural inorganic sorbent (pemza) for removal of Cr(VI) ions from water resources, V International Conference Ecology of Urban Areas, (2016) 109.
8. Memedi H., Atkovska K., Lisichkov K., Marinkovski M., Bozinovski Z., Kuvendziev S., Reka A.A., Memedi, H., Investigation of the possibility for application of natural inorganic sorbent (aksil) for heavy metals removal from water resources, 2nd International and 6th Croatian Scientific and Professional Conference Water for all, (2016) 185-192.
9. Reka A.A., Anovski T., Bogoevski S., Pavlovski B., Boškovski B., Physical-chemical and mineralogical-petrographic examinations of diatomite from deposit near village of Rožden, Republic of Macedonia, Geologica Macedonica, 28 (2014) 121-126.
10. Reka, A., Pavlovski, B., Boev, B., Boev, I., Makreski, P., (2018): Chemical, mineralogical and structural characterization of diatomite from Republic of Macedonia. In: 17th Serbian Geological Congress, 17-20 May 2018, Vrnjačka Banja, Serbia.
11. Cekova B., Pavlovski B., Spasev D., Reka A., Structural examinations of natural raw materials pumice and trepel from Republic of Macedonia, Proceedings of the XV Balkan Mineral Processing Congress, Sozopol, Bulgaria, (2013) 73-75.
12. Reka A. A., Durmishi B., Jashari A., Pavlovski B., Buxhaku Nj., Durmishi A., Physical-Chemical and Mineralogical-Petrographic Examinations of Trepel from Republic of Macedonia, IJISSET, 2 (2016) 13-17.
13. Pavlovski B., Jančev S., Petreski L., Reka A., Bogoevski S., Boškovski B., Trepel – a peculiar sedimentary rock of biogenetic origin from the Suvodol village, Bitola, R. Macedonia, Geologica Macedonica, 25 (2011) 67-72.
14. Bogoevski, S., Jančev, S., Boškovski, B., Characterization of Diatomaceous Earth from Slavishko Pole locality in the Republic of Macedonia, Geologica Macedonica, 28 (1) (2014) 39-43.
15. Reka, A. A., Pavlovski, B., Boev, B., Bogoevski, S., Boškovski, B., Lazarova, M., Lamamra, A., Jashari, A., Jovanovski, G., & Makreski, P.. Diatomite – evaluation of physico-mechanical, chemical, mineralogical and thermal properties. Geologica Macedonica, 35(1) (2021) 5-14.
16. Reka, A., Pavlovski, B., Fazlija, E., Berisha, A., Pacarizi, M., Daghmehchi, M., Sacalis, C., Jovanovski, G., Makreski, P. & Oral, A.. Diatomaceous Earth: Characterization, thermal modification, and application. Open Chemistry, 19(1) (2021) 451-461.
17. Memedi H, Reka A.A., Kuvendziev S. Atkovska K., Garai M., Marinkovski M., Pavlovski B., Lisichkov K., Chapter 3 - Adsorption of Cr(VI) ions from aqueous solutions by diatomite and clayey diatomite, Editor(s): Sunil Kumar, Muhammad Zaffar Hashmi, In Advances in Pollution Research, Biological Approaches to Controlling Pollutants, Woodhead Publishing, 2022, Pages 29-48, ISBN 9780128243169, https://doi.org/10.1016/B978-0-12-824316-9.00002-1.
18. Memedi H, Atkovska K, Kuvendziev S, Garai M, Marinkovski M, Dimitrovski D, et al. Removal of Chromium(vi) from aqueous solution by clayey diatomite: kinetic and equilibrium study. In: Stafilov T., Balabanova B., editors. Contaminant levels and ecological effects – understanding and predicting with chemometric methods,

Springer, Switzerland, (2021) 263-282.
19. Šaponjić A., Gyoshev S., Baščarević Z., Janković Mandić Lj., Ljubenov G., Kokunešoski M., Characterization of Sedimentary Minerals from Kolubara Mining Basin, Serbia, with the Determination of Natural Radioactivity, Science of Sintering, 54 (2022) 39-48.
20. Eldernawi A.M., Rious J.M., Al-Samarrai K.I., Chemical Physical and Mineralogical Characterization of Al-Hishal Diatomite at Subkhah Ghuzayil Area Libya, International Journal of Research Applied, Natural and Social Sciences, 2(2014) 165-174.
21. Smirnov P.V., Konstantinov A.O., Gursky H.-J., Petrology and industrial application of main diatomite deposits in the Transuralian region (Russian Federation), Environmental Earth Sciences, (2017) 676-682.
22. Ediz, N., Bentli, İ., Tatar, İ., Improvement in filtration characteristics of diatomite by calcination, International Journal of Mineral Processing, 94 (2010) 129-134.
23. Ilia I.K., Stamatakis M.G., Perraki Th.S., Mineralogy and technical properties of clayey diatomites from north and central Greece, Central European Journal of Geosciences, 1 (2009) 393-403.
24. S. Nenadović, Lj. Kljajević1, S. Marković, M. Omerašević,U. Jovanović, V. Andrić, I. Vukanac, Natural Diatomite (Rudovci, Serbia) as Adsorbent for Removal Cs from Radioactive Waste Liquids, Science of Sintering, 47 (2015) 299-309.
25. Athar S.D., Hasan Asilian H., Catalytic Oxidation of Carbon Monoxide Using Copper-Zinc Mixed Oxide Nanoparticles Supported on Diatomite, J Health Scope, 1 (2012) 52-56.
26. Manevich V.E., Subbotin R.K., Nikiforov E.A., Senik N. A., Meshkov A.V., Diatomite - siliceous material for the glass industry, Glass and Ceramics, 69 (2012) 168-172.
27. Akhtar F., Rehman Y., Bergström L., A study of the sintering of diatomaceous earth to produce porous ceramic monoliths with bimodal porosity and high strength, Powder technology, 201 (2010) 253-257.
28. Reka A.A., Pavlovski B., Makreski P., New optimized method for low-temperature hydrothermal production of porous ceramics using diatomaceous earth, Ceramics international, 43 (2017) 12572-12578.
29. Reka A., Pavlovski B., Incluence of the nature of silica on physical and mechanical properties of lightweight silicate bonded building products obtained by hydrothermal treatment, Book of Abstracts of the XVIII Congress of Chemists and Technologists of Macedonia, Ohrid, Macedonia, 2004, 78.
30. Pavlovski B., Zafirovski S., Zlatanovic V., Lightweight ceramic construction materials with hydrosilicate bonding, Proceedings of the VII Yugoslavian Congress for Chemistry and Technology, Novi Sad, Yugoslavia, 1983, 77-81.
31. Pavlovski B., Buntevska V., Lightweight ceramic materials obtained by hydrothermal procedure, Book of Abstracts of the XVI Congress of Chemists and Technologists of Macedonia, Skopje, Macedonia, 1999, 96.
32. Reka A., Influence of mineralogical composition and microstructure of the binding material on the physico-mechanical properties of ceramic products obtained by hydrothermal process [dissertation]. Skopje (MK): Ss. Cyril and Methodius University; 2004.
33. Reka A.A., Synthesis and characterization of porous SiO2 ceramics obtained from diatomite with the use of low-temperature hydrothermal technology [dissertation]. Skopje (MK): Ss. Cyril and Methodius University; 2016.
34. Yılmaz B., Ediz N., The use of raw and calcined diatomite in cement production, Cement and Concrete Composites, 30 (2008) 202-211.

35. Maja Kokunešoski, Miroslav Stanković, Marina Vuković, Jelena Majstorović, Đorđe Šaponjić, Svetlana Ilić, Aleksandra Šaponjić, Macroporous Monoliths Based on Natural Mineral Sources, Clay and Diatomite, Science of Sintering, 52 (2020) 339-348.
36. Fragoulis D., Stamatakis M.G., Papageorgiou D., Chaniotakis E., The physical and mechanical properties of composite cements manufactured with calcareous and clayey Greek diatomite mixtures, Cement and Concrete Composites, 27 (2005) 205-209.
37. Rahimov R.Z., Kamalova Z.A., Ermilova E.J.O, Stojanov V., Thermally treated trepel as active mineral additive in cement, Gazette of Kazan Institute of Technology, 17 (2014) 99-101.
38. Kastis D., Kakali G., Tsivilis S., Stamatakis M.G., (2006). Properties and hydration of blended cements with calcareous diatomite, Cement and Concrete Research, 36 (2006) 1821-1826.
39. Loganina V.I., Simonov E.E., Jezierski W., Małaszkiewicz D., Application of activated diatomite for dry lime mixes, Constructions and Building Materials, 65 (2014) 29-37.
40. Mota dos Santos A.A., Cordeiro G.C., Investigation of particle characteristics and enhancing the pozzolanic activity of diatomite by grinding, Materials Chemistry and Physics, 270(2021) 124799.
41. Paules D., Hamida S., Lasheras R. J., Escudero M., Benouali D., Cáceres J.O., Anzano J., Characterization of natural and treated diatomite by laser-induced breakdown spectroscopy (LIBS), Microchemical Journal, 137 (2018) 1-7.
42. Vu D.-H., Wang K.-S., Bac B. H., Nam B. X., Humidity control materials prepared from diatomite and volcanic ash, Construction and Building Materials, 38 (2013) 1066-1072.
43. Janićijević J., Krajišnik D., Čalija B., Dobričić V., Daković A., Krstić J., Marković M., Milić J., Inorganically modified diatomite as a potential prolonged-release, Materials Science and Engineering C, 42 (2014) 412-420.
44. Inglethorpe S.D.J., Industrial Minerals Laboratory Manual: Diatomite, British Geological Survey, 1-46, 1993.
45. Reka A, Pavlovski B, Boev B, Boev I, Makreski P. Phase transitions of silica in diatomite from Besiste (North Macedonia) during thermal treatment. Proceedings of the II geology congress of Bosnia and Herzegovina, Geological society of Bosnia and Herzegovina, Laktaši, Bosnia and Herzegovina; 2019 Oct 2–4. p. 166–8.
46. Zheng R., Ren Z., Gao H., Zhang A., Bian, Z., Effects of calcination on silica phase transition in diatomite, Journal of Alloys Compounds, 757 (2018) 364-371.
47. Gulturk E., Guden M., Thermal and acid treatment of diatom frustules, Journal of Achievements of Materials and Manufacturing Engineering, 46 (2011) 196-203.
48. Ibrahim S.S., Selim A.Q., Heat treatment of natural diatomite, Physicochemical Problems of Mineral Processing, 48 (2012) 413-424.
49. Loganina V.I., Simonov E.E., Jezierski W., Małaszkiewicz D., Application of activated diatomite for dry lime mixes, Construction and Building Materials, 65 (2014) 29-37.
50. Reka A.A., Pavlovski B., Anovski T., Bogoevski S., Boškovski B., Phase transformations of amorphous SiO_2 in diatomite at temperature range of 1000–1200°C, Geologica Macedonica, 29 (2015) 87-92.
51. Reza A.P.S., Hasan A.M., Ahmad J.J., Zohreh F., Jafar T., The Effect of Acid and Thermal Treatment on a Natural Diatomite, Chemistry Journal, 1 (2015) 144-150.
52. Aguedal H., Hentit H., Merouani D.R., Iddou A., Shishkin A., Jumas J.C., Improvement of the Sorption Characteristics of Diatomite by Heat Treatment, Key Engineering Materials, 721 (2017) 111-116.

53. Reka A.A., Pavlovski B., Ademi E., Jashari A., Boev B. Boev I., Makreski P., Effect of Thermal Treatment of Trepel at Temperature Range 800-1200^{o}C, Open Chemistry, 17 (2019) 1235-1243.
54. Chukanov N.V., Infrared spectra of mineral species, Springer Geochemistry/Mineralogy, 2014.
55. Chen F., Miao Y., Ma L., Zhan F., Wang W., Chen N., Xie Q., Optimization of pore structure of a clayey diatomite, Particulate Science and Technology, (2019) 1-7.

Сажетак: *Сирова дијатомејска земља из околине Битоља (Северна Македонија) показала је ниску насипну густину (0,61–0,69 g/cm^3), високу апсорпцију воде (75–81%) и порозност (66–72%). Хемијски састав је одређен помоћу ИЦП-МС, откривајући следеће резултате за дијатомејску земљу SiO_2 (63.69 wt%), Al_2O_3 (11.79 wt%), Fe_2O_3 (5.95 wt%), MnO (0.15 wt%), TiO_2 (0.65 wt%), CaO (1.51 wt%), MgO (2.24 wt%), P_2O_5 (0.13 wt%), K_2O (1.64 wt%), Na_2O (0.93 wt%), LOI (11.21 wt%). XRPD подаци испитиваног узорка глиненог дијатомита углавном су приказали кристално понашање са малим присуством аморфне фазе. Кристалне минералне фазе углавном обухватају: силицијум диоксид (кварц), фелдспат (плагиоклас), лискун (московит), хлорите и доломит. Резултати СЕМ и ТЕМ показали су присуство микро- и нано структура са порама у распону од 250 до 600 nm. Глинени дијатомит је синтерован на три температуре (900ºC, 1000ºC и 1100ºC) у трајању од 1 сата. КСРПД синтерованих узорака на 1100ºC показао је извесну термичку стабилност и формирање нових фаза (мулит и тридимит) што чини анализирану дијатомејску земљу погодном за производњу разних врста керамичких, грађевинских и термоизолационих материјала.*
Кључне речи: *Диатомејска земља, минерали глине, карактеризација, синтеровање.*